CDF/PHYS/EXOTIC/PUBLIC/11110

Search for New Resonances Decaying to a Top and a Bottom Quark in $p\bar{p}$ Collisions at $\sqrt{s} = 1.96$ TeV

The CDF Collaboration[1]

[1] *URL http://www-cdf.fnal.gov*

(Dated: September 10, 2014)

Abstract

This note reports on a search for W'-like resonances decaying to tb in the full data set of proton-antiproton collisions at $\sqrt{s} = 1.96$ TeV recorded by the CDF II detector at the Tevatron, corresponding to an integrated luminosity of 9.5 fb^{-1}. No significant excess above SM prediction is found. Using a benchmark $W' \to tb$ left-right symmetric model, we place 95% C.L. mass-dependent upper limits on the W' production cross section times branching ratio to tb. Assuming a W' with SM-like couplings and allowed (forbidden) decay to leptons, we exclude $W' \to tb$ for W' masses below 860 (880) GeV/c^2. Relaxing the hypothesis on SM-like couplings, we exclude W' boson coupling strength values $g_{W'}$ as a function of W' mass down to $g_{W'} = 0.4 g_{\rm SM}$ for $M_{W'} = 300$ GeV/c^2. Our limits are significantly stronger than the LHC ones below $M_{W'}$ around 750 GeV/c^2, and extend to W' masses as low as 300 GeV/c^2.

INTRODUCTION

Several modifications of the Standard Model (SM) of particle physics include massive, short-lived states decaying to pairs of SM leptons or quarks. A resonance decaying to a top and a bottom quark tb (where tb indicates both the state $t\bar{b}$ and its charge conjugate $\bar{t}b$) can appear in models featuring one or more massive charged vector bosons, generically denoted as W', such as $SU(2)_R$ SM extensions [1], Kaluza-Klein extra-dimensions [2, 3], technicolor [4, 5] or Little Higgs scenarios [6]. Searches for W' bosons in the $W' \to tb$ decay channel are complementary to searches in the leptonic decay channel $W' \to \ell\nu$, and can probe cases where the couplings of the W' to fermions are free parameters.

In the recent past, searches in the $W' \to tb$ channel have been performed by the CDF [7] and D0 [8] experiments at the Tevatron, and by the ATLAS [9] and CMS [10] experiments at the LHC. For resonance searches at the highest masses, the LHC experiments have superior sensitivity to the Tevatron due to the higher center-of-mass energy. However, in the lower mass region ($M_{W'} < 700$ GeV/c^2) the Tevatron experiments have competitive sensitivity due to the more favorable signal-to-background ratio in searches for particles produced in quark-initiated states, such as the W', with respect to the SM background processes which are mainly gluon initiated.

In this Letter we present a new search for W'-like resonances decaying to tb in events where $t \to Wb$ and the W decays to a charged lepton-neutrino pair.

A simple left-right symmetric SM extension [11], predicting the existence of W' bosons of unknown mass and universal weak coupling strength to SM fermions, is used as a benchmark model. Since no specific assumptions on the signal model are made throughout the analysis, this search is sensitive to any narrow resonant state decaying to tb.

EVENT SELECTION

The collision events analyzed in this search were produced at the Tevatron $p\bar{p}$ collider at a center-of-mass energy of 1.96 TeV and were recorded by the CDF II detector [12]. The CDF II detector consists of high-precision tracking systems for vertex and charged-particle track reconstruction, surrounded by electromagnetic and hadronic calorimeters for energy measurement, and muon subsystems outside the calorimeter for muon detection. CDF II

uses a cylindrical coordinate system with azimuthal angle ϕ, polar angle θ measured with respect to the positive z direction along the proton beam, and the distance r measured from the beamline. The pseudorapidity, transverse energy, and transverse momentum are defined as $\eta = -\ln\left[\tan(\frac{\theta}{2})\right]$, $E_T = E\sin\theta$, and $p_T = p\sin\theta$, respectively, where E and p are the energy and momentum of an outgoing particle. The missing transverse energy $\vec{\not\!\!E}_T$ is defined by $\vec{\not\!\!E}_T = -\sum_i E_T^i \hat{n}_i$, where $\hat{n}_i$ is a unit vector perpendicular to the beam axis that points to the i^{th} calorimeter tower ($\not\!\!E_T = |\vec{\not\!\!E}_T|$).

Events are accepted by the online event selection (trigger) that requires $\not\!\!E_T > 45$ GeV or, alternatively, $\not\!\!E_T > 35$ GeV and two or more jets with transverse energy $E_T > 15$ GeV, forming the *emet* datastream. The efficiency associated with this selection is obtained from data and is applied to the Monte-Carlo (MC) simulated samples to reproduce the efficiencies of the data. The parametrization of the trigger efficiency [13] significantly improves the modeling of the trigger turn-on outside the fully efficient region, as verified using data control samples. The full CDF dataset, corresponding to an integrated luminosity of 9.5 fb^{-1}, is analyzed. The qcd si GR- LvHiggs list of good runs are used, which includes runs recovered from all data periods.

The event selection applied in this search is similar to the s-channel single-top-quark search reported in Ref.[14]. Since we are looking for massive resonances decaying in a t and in a b quark the minimum values required for the $\not\!\!E_T$ and jet energies are higher with respect to the selection critiria used in the s-channel analysis. Also, in order to include events containing identified electrons or muons, the lepton veto included in the s-channel search is removed. Offline, $\not\!\!E_T > 50$ GeV is required, after correcting measured jet energies for instrumental effects [15]. Events with two or three high-E_T jets are selected and the two jets with the largest transverse energies, $E_T^{j_1}$ and $E_T^{j_2}$, are required to satisfy $E_T^{j_1} > 35$ GeV and $E_T^{j_2} > 25$ GeV, where the jet energies are determined from calorimeter deposits corrected by track momentum measurements [16]. Some of these events consist of signal candidates in which the tau lepton from the $t \to Wb \to \tau\nu b$ decay is reconstructed as a jet in the calorimeters. To increase the acceptance for events with an unidentified τ lepton, events in which the third-most energetic jet satisfies $E_T^{j_3} > 15$ GeV are accepted. Because of the large rate of inclusive quantum chromodynamics (QCD) multijet (MJ) production, events with four or more reconstructed jets, where each jet has transverse energy in excess of 15 GeV and pseudorapidity [17] $|\eta| < 2.4$, are rejected. To ensure that the two leading-E_T

jets are within the silicon-detector acceptance, they are required to satisfy $|\eta| < 2$, with at least one of them satisfying $|\eta| < 0.9$.

The MJ background events most often contain $\not\!\!E_T$ generated through jet energy mismeasurements. Neutrinos produced in semileptonic b-hadron decays can also contribute to the $\not\!\!E_T$ of these events. In both cases, the $\vec{\not\!\!E}_T$ is typically aligned with $\vec{E}_{\rm T}^{j_2}$ (or $\vec{E}_{\rm T}^{j_3}$, for events with a third jet), and events are rejected by requiring the azimuthal separation between $\vec{\not\!\!E}_T$ and $\vec{E}_{\rm T}^{j_2}$ (or $\vec{E}_{\rm T}^{j_3}$) to be larger than 0.4. The events that satisfy the requiremts listed above form the *pretag* sample. At this stage of the analysis, 941.12 signal events, simulated considering a W' mass of 300 GeV, are accepted by the selection, compared to a total number of data events of 391,229. In order to identify jets originated from the fragmentation of a hadron containing a b-quark ("b-tagging"), two different algorithms are used: SECVTX [12], a tight (T) algorithm, and JETPROB [18], a loose (L) algorithm. The choice to use SECVTX and JETPROB insted of the HOBIT tagger used in Ref. [14] is due to the fact that we expect in this search a large contribution from events with high energetic jets while HOBIT is not able to distinguish light-flavor jets for heavy-flavor jets if the jet energy is larger than 200 GeV.

At least one of the first two leading jets in E_T is required to be tagged by SECVTX. Events are further divided among twelve statistically independent regions, depending on whether the other leading jet is not tagged (Exclusive 1 Tight, 1T), tagged by JETPROB but not by SECVTX (1 Tight + 1 Loose, TL), and tagged by SECVTX (2 Tight, TT); the number of jets (two-jet or three-jet sample) and the presence of at least one reconstructed electron or muon (no-lepton and lepton sample) This division results in an increased sensitivity because signal-to-noise ratio and background composition are different among the analysis subsamples. Events satisfying the aforementioned requirements comprise the *preselection* sample. At this stage of the analysis 483.4 signal events for a W' mass of 300 GeV, are accepted by the selection, compared to a total number of data events of 25,256.

SIGNAL AND BACKGROUND MODEL

The most important contribution to the preselection sample is due to multijet production from strong interactions (QCD multijet). Other processes giving significant contributions are: top-antitop quark pair production ($t\bar{t}$), electroweak single top production, dibosons

(WW/WZ), and production of jets in association with a W or Z boson (W/Z + jets), including both heavy-flavor jets (from b or c quarks) and jets from light-flavor quarks which have been erroneously b-tagged. A combination of Monte Carlo simulations and data-driven techniques are used to derive the models for SM background processes.

The kinematic distributions of events associated with top-quark pair, single top quark, V+jets (where V stands for a W or a Z boson), $W + c$, diboson (VV) and associated Higgs and W or Z boson (VH) production are modeled using simulations. The ALPGEN generator [19] is used to model V+jets at leading order (LO) with up to four partons based on generator-to-reconstructed-jet matching [20, 21], and $W + c$. The POWHEG [22] generator is used to model t- and s-channel single top quark production, while PYTHIA [23] is used to model top-quark-pair, VV, and VH production at LO. Each event generator uses the CTEQ5L parton distribution functions [24] as input to the simulations. Parton showering is simulated in all cases using PYTHIA, tuned to the Tevatron underlying-event data [25]. Event modeling also includes simulation of the detector response using GEANT [26]. The simulated events are reconstructed and analyzed in the same way as the experimental data. Normalizations of the event contributions from t- and s-channel single top quark, VV, VH, and $t\bar{t}$ pair production are taken from theoretical cross section predictions [27–30], while normalization for $W + c$ production is taken from the measured cross section [31]. For V+jets production, the heavy-flavor contribution is normalized based on the number of b-tagged events observed in an independent data control sample [32]. Contributions of V+jets and VV events containing at least one incorrectly b-tagged light-flavored jet, are determined by applying to simulated events per-event mistag probabilities, obtained from a generic event sample containing light-flavored jets [33, 34], to simulated events.

QCD multijet events are difficult to simulate. For this reason, a QCD multijet background model is derived from data in an independent data sample composed of events with $\Delta\varphi(\vec{\not\!\!E}_T, \vec{E}_{\mathrm{T}}^{j_2}) < 0.4$ and $50 < \not\!\!E_T < 70$ GeV, consisting almost entirely of QCD multijet contributions. First, a probability density function f_i is formed separately in each b-tagging subsample i (i = 1T, TL, TT) by taking the ratio between tagged and pretagged events as a function of several variables, as described in detail in [35]. Then, a QCD multijet template is determined separately for each region i by weighting the untagged data in the preselection sample according to the probability density functions f_i.

The signal model is a W' with purely right-handed decays, simulated using PYTHIA for W' mass $M_{W'}$ in the range $300 \leq M_{W'} \leq 900$ GeV/c^2in 100 GeV/c^2increments. As the W' helicity does not affect analysis observables, this model is valid for both a right-handed and a left-handed W' under the assumption of no interference with SM W. Two different scenarios are considered, depending on whether the leptonic decay mode $W' \to \ell\nu$ is allowed or forbidden. The latter, for instance, is the case if the right-handed neutrino ν_R is more massive than the W'. The only effect of the forbidden leptonic decay mode is an increased branching fraction $\mathcal{B}(W' \to tb)$.

As an intermediate background rejection step, an Artificial Neural Network, $\mathrm{NN_{QCD}}$, is employed to separate the dominant QCD multijet background from signal and other backgrounds. $\mathrm{NN_{QCD}}$ is a feed-forward multilayer perceptron, bearing activity-derived ($\not\!\!E_T$, $\not\!\!p_T$[36]), angular ($\Delta\varphi(\vec{\not\!\!E}_T, \vec{\not\!\!p}_T)$, angular separations between $\vec{\not\!\!E}_T$, $\vec{\not\!\!p}_T$ and jet directions), and event-shape (sphericity [37]) observables. We have employed the same $\mathrm{NN_{QCD}}$ function constructed to separate W+jets events from background in the s-channel single-top-quark search. This is justified because the final state topologies between W' and s-channel single-top-quark production are very similar. As no information on the W' mass is included in the training sample, this also ensures a consistent performance in QCD multijet background separation across the whole W' mass hypothesis range.

Events are required to satisfy a minimum $\mathrm{NN_{QCD}}$ requirement, forming the *signal* region. To determine the appropriate normalization in each different analysis subsample, a scale factor is derived in the region composed by the rejected events, where the tagged diboson, top and W/Z + jets background estimates are subtracted from the tagged data. Table IV shows expected event yields for background processes, observed data events, and expected number of events for one signal hypothesis.

A staged neural network techinique is applied to derive a final discriminant to distinguish each W' mass hypothesis from the remaining backgrounds. Two additional networks, $\mathrm{NN}_{V\mathrm{jets}}$ and $\mathrm{NN}_{t\bar{t}}$, are trained for events that satisfy the minimum requirement on the $\mathrm{NN_{QCD}}$ output variable. The first, $\mathrm{NN}_{V\mathrm{jets}}$, is trained to separate the W' signal from V+jets and the remaining QCD backgrounds. In the training, a simulated W' signal is used, while the background sample consists of pretag data events that satisfy the requirement on $\mathrm{NN_{QCD}}$, reweighted by the probability for an event to be b-tagged (tag-rate probability) as derived from the tag-rate matrix. The second, $\mathrm{NN}_{t\bar{t}}$, is trained to separate W' from $t\bar{t}$ production

using simulation for both components. Variables which describe the energy and momentum flow in the detector and angular variables are used in the training of the $\mathrm{NN}_{V\mathrm{jets}}$ and $\mathrm{NN}_{t\bar{t}}$ discriminants. The final discriminant, $\mathrm{NN}_{\mathrm{sig}}$, is defined as the quadrature sum of the $\mathrm{NN}_{V\mathrm{jets}}$ and $\mathrm{NN}_{t\bar{t}}$ output variables, both weighted by an appropritate weight optimized to improve the sensitivity in each analysis subsample, taking into account the differing background contributions.

TABLE I. Numbers of predicted and observed two-jet no-lepton events in the 1T, TL, and TT subsamples. The uncertainties on the predicted numbers of events are due to the theoretical-cross-section uncertainties and the uncertainties on signal and background modeling. Expected number of events for one choice of W' mass and $\sigma(p\bar{p} \to W') \times \mathcal{B}(W' \to tb)$ is also shown.

Category	1T	TL	TT
$M_{W'} = 300$ GeV/c^2	102.9 ± 8.9	38.8 ± 4.0	54.1 ± 6.9
s-ch single top	66.2 ± 8.8	24.0 ± 3.4	30.2 ± 3.8
t-ch single top	114.0 ± 21.8	5.0 ± 1.0	5.2 ± 1.0
$t\bar{t}$	215.2 ± 21.6	56.4 ± 6.2	68.9 ± 6.3
VV	186.3 ± 16.8	21.4 ± 1.9	20.3 ± 1.9
VH	10.0 ± 1.1	3.8 ± 0.5	5.1 ± 0.5
V+jets	2787.1 ± 874.6	190.5 ± 59.4	118.1 ± 36.8
QCD	2543.9 ± 63.1	191.3 ± 12.6	93.3 ± 9.1
Total background	5922.8 ± 877.6	492.4 ± 61.1	341.2 ± 38.7
Observed	5772	477	323

LIMITS EXTRACTION

A binned likelihood fit is performed to probe for a $W' \to tb$ signal in the presence of SM backgrounds. The likelihood is the product of Poisson probabilities over the bins of the $\mathrm{NN}_{\mathrm{sig}}$ distribution. The mean number of expected events in each bin includes contributions from each background source and from the $W' \to tb$ process assuming a given value of $M_{W'}$. The method employed is a Bayesian likelihood method [38] with a flat, non-

TABLE II. Numbers of predicted and observed two-jet lepton events in the 1T, TL, and TT subsamples.

Category	1T	TL	TT
$M_{W'} = 300$ GeV/c^2	53.2 ± 4.6	21.1 ± 2.2	30.5 ± 3.9
s-ch single top	32.1 ± 4.3	12.4 ± 1.7	15.9 ± 2.0
t-ch single top	53.0 ± 10.2	2.3 ± 0.4	2.7 ± 0.5
$t\bar{t}$	242.2 ± 24.2	84.5 ± 9.2	108.5 ± 9.8
VV	72.9 ± 6.6	7.1 ± 0.7	6.7 ± 0.6
VH	4.0 ± 0.4	1.6 ± 0.2	2.1 ± 0.2
V+jets	685.4 ± 215.1	45.9 ± 14.3	38.6 ± 12.1
QCD	222.2 ± 81.0	28.7 ± 11.1	8.2 ± 8.2
Total background	1311.9 ± 231.5	182.4 ± 20.4	182.7 ± 18.0
Observed	1356	203	184

TABLE III. Numbers of predicted and observed three-jet no-lepton events in the 1T, TL, and TT subsamples.

Category	1T	TL	TT
$M_{W'} = 300$ GeV/c^2	57.7 ± 5.0	17.4 ± 1.8	21.4 ± 2.8
s-ch single top	37.4 ± 5.0	9.9 ± 1.4	12.1 ± 1.5
t-ch single top	67.3 ± 12.9	4.1 ± 0.8	4.8 ± 0.9
$t\bar{t}$	547.0 ± 54.7	87.8 ± 9.6	94.0 ± 8.5
VV	83.4 ± 7.6	7.9 ± 0.7	6.3 ± 0.6
VH	4.8 ± 0.5	1.3 ± 0.2	1.6 ± 0.2
V+jets	1108.1 ± 347.7	66.5 ± 20.7	41.5 ± 13.0
QCD	1174.9 ± 32.6	80.3 ± 5.9	29.9 ± 4.2
Total background	3022.9 ± 353.9	257.6 ± 23.7	190.1 ± 16.2
Observed	2934	279	189

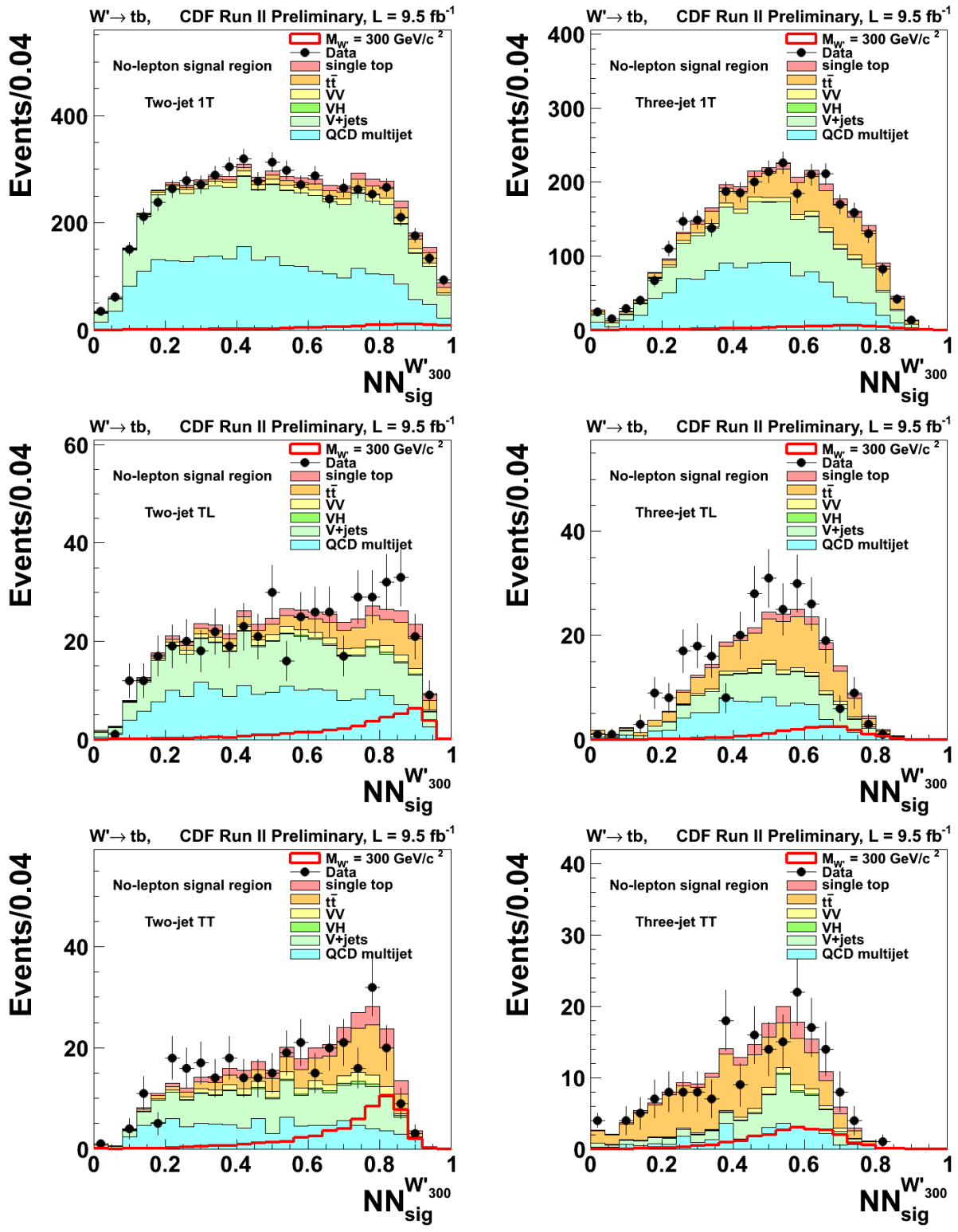

FIG. 1. Predicted and observed final discriminant distributions in the no-lepton signal region, for (a) 1T two-jet, (b) 1T three-jet, (c) TL two-jet, (d) TL three-jet, (e) TT two-jet and (f) TT three-jet event subsamples.

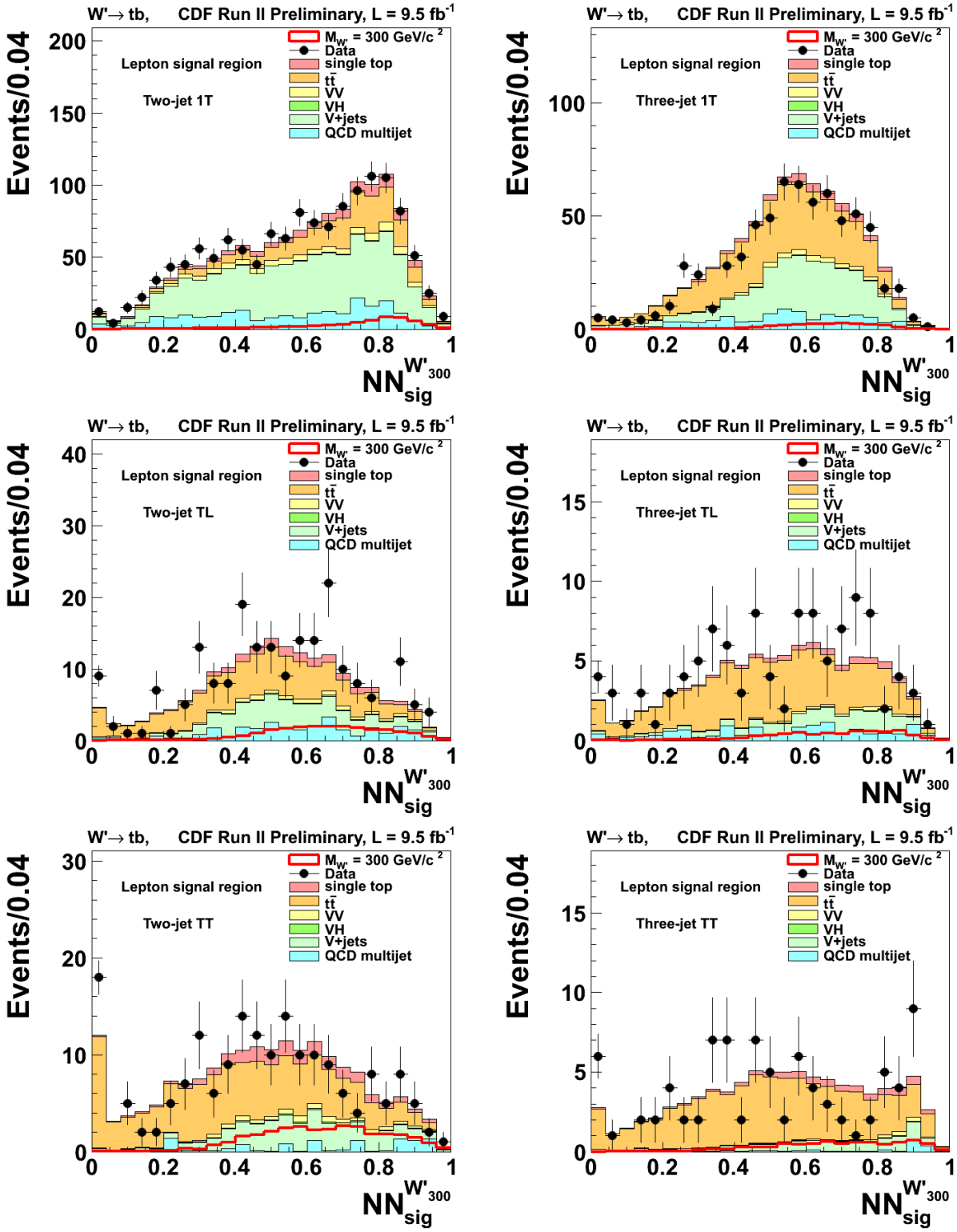

FIG. 2. Predicted and observed final discriminant distributions in the lepton signal region, for (a) 1T two-jet, (b) 1T three-jet, (c) TL two-jet, (d) TL three-jet, (e) TT two-jet and (f) TT three-jet event subsamples.

TABLE IV. Numbers of predicted and observed three-jet lepton events in the 1T, TL, and TT subsamples.

Category	1T	TL	TT
$M_{W'} = 300$ GeV/c^2	21.8 ± 1.9	6.1 ± 0.7	7.4 ± 1.0
s-ch single top	12.6 ± 1.7	3.1 ± 0.4	3.9 ± 0.5
t-ch single top	23.5 ± 4.5	1.7 ± 0.3	2.1 ± 0.4
$t\bar{t}$	352.7 ± 35.3	60.4 ± 6.6	67.6 ± 6.2
VV	23.0 ± 2.2	1.8 ± 0.2	1.5 ± 0.2
VH	1.5 ± 0.2	0.4 ± 0.0	0.5 ± 0.1
V+jets	251.8 ± 79.0	14.1 ± 4.4	10.1 ± 3.2
QCD	86.3 ± 55.5	12.5 ± 7.3	1.9 ± 1.9
Total background	751.3 ± 103.0	94.1 ± 10.8	87.7 ± 7.3
Observed	679	109	85

negative, prior probability for the W' boson production cross section times branching fraction, $\sigma(p\bar{p} \to W') \times \mathcal{B}(W' \to tb)$, and truncated Gaussian priors for the uncertainties on the acceptance and shape of the backgrounds. We combine the three b-tagging regions by taking the product of their likelihoods and simultaneously varying the correlated uncertainties.

Systematic uncertainties considered in the fit include both uncertainties on template normalization, and uncertainties on the shape of the $\mathrm{NN_{sig}}$distribution. Uncertainties due to the same source are considered 100% correlated. These uncertainties, which apply to both signal and backgrounds, include luminosity measurement (6%), b-tagging efficiency (8 to 16%), trigger efficiency (1 to 3%), lepton veto efficiency (2%), parton distribution functions (3%), and up to 6% for the jet-energy scale [15] . Initial- and final-state radiation uncertainties (2%) are applied only to top processes ($t\bar{t}$and single top).

The uncertainties due to finite simulations statistics, and the uncertainties on the normalization of $t\bar{t}$(3.5%), t-channel single top quark (6.2%), s-channel single top quark (5%), diboson (6%) from the theoretical cross-section calculations [27, 28, 30], $W + c$ (23%) from the measured cross section [29, 31], and QCD multijet (3 to 100%, calculated from scale

factors) are not correlated. The rates of production of events with a W or a Z boson plus heavy-flavor jets are associated with 30% uncertainty.

The shapes obtained by varying the probability density functions f_i by one standard deviation from their central values are applied as uncertainties on the shapes of the QCD background. Changes in the shape of the $\mathrm{NN_{sig}}$ distribution originating from jet energy scale uncertainties are also incorporated for processes modeled via the simulation.

An additional uncertainty on the b-tagging efficiency is applied to signal templates as an E_T-dependent term, to properly take into consideration the uncertainty in the extrapolation of the b-tagging scale factor to the high-E_T regions typical of $W' \to tb$ events.

The aforementioned procedure is carried out for all signal mass hypotheses, obtaining 95% C.L. upper limits on $\sigma(p\bar{p} \to W') \times \mathcal{B}(W' \to tb)$ as a function of $M_{W'}$, using the methodology described in Ref. [32]. The expected and observed upper limits are shown in Figure 3. The observed limits are compatible with the expectations calculated assuming that no $W' \to tb$ signal is present in the data. By comparing the limits on $\sigma(p\bar{p} \to W') \times \mathcal{B}(W' \to tb)$ with the theoretical NLO calculations for a right-handed W' with SM-like couplings [11], we exclude W' bosons for masses less than 860 (880) GeV/c^2in cases where decay to leptons is allowed (forbidden).

For a simple s-channel production model with effective coupling $g_{W'}$, the cross-section is proportional to $g^4_{W'}$. Relaxing the assumption of universal weak coupling, the limits on the cross-section can be interpreted as upper limits on $g_{W'}$ as a function of $M_{W'}$. The excluded region of the $g_{W'}$–$M_{W'}$ plane is shown in Figure 4, with $g_{W'}$ expressed in units of g_{SM}. For a value of $M_{W'} = 300$ GeV/c^2, the effective coupling is constrained at the 95% C.L. to be less than 0.4 of the W boson coupling.

RESULTS

In conclusion, we have performed a search for a massive resonance decaying to tb in the $\not\!\!E_T$plus jets final state with the full CDF II dataset, corresponding to an integrated luminosity of 9.5 fb^{-1}. The data are found to be consistent with the background-only hypothesis, and upper limits are set on the production cross-section times branching ratio at the 95% confidence level. For a specific benchmark model (left-right symmetric SM extension), in cases where the leptonic decay mode is allowed (forbidden), we exclude W'

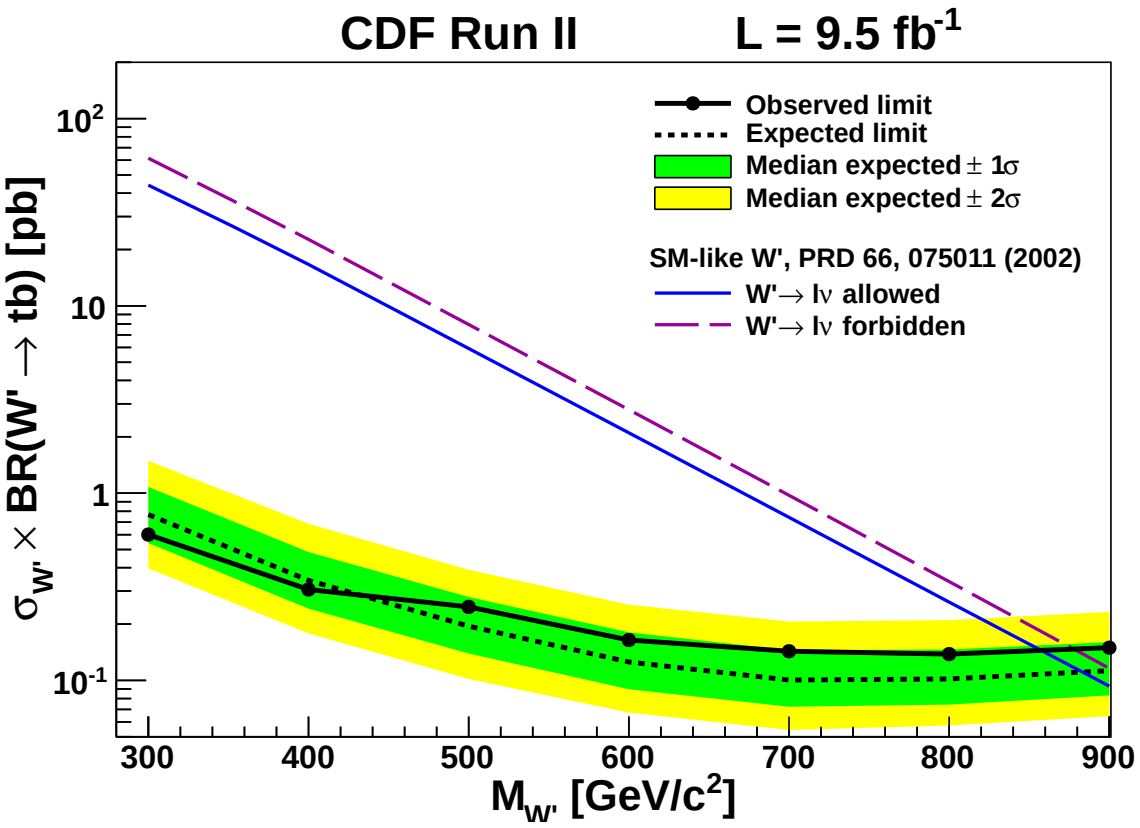

FIG. 3. Observed and expected limits on $\sigma(p\bar{p} \to W') \times \mathcal{B}(W' \to tb)$, with $\pm 1\sigma$ and $\pm 2\sigma$ confidence intervals and theoretical predictions for a right-handed W' with SM-like couplings in cases where the leptonic decay mode $W' \to \ell\nu$ is allowed (solid line) or forbidden (dashed).

bosons with masses lower than 860 (880) GeV/c^2. For masses smaller than approximately 700 GeV/c^2, this search yields the most constraining limits to date on narrow tb resonances production.

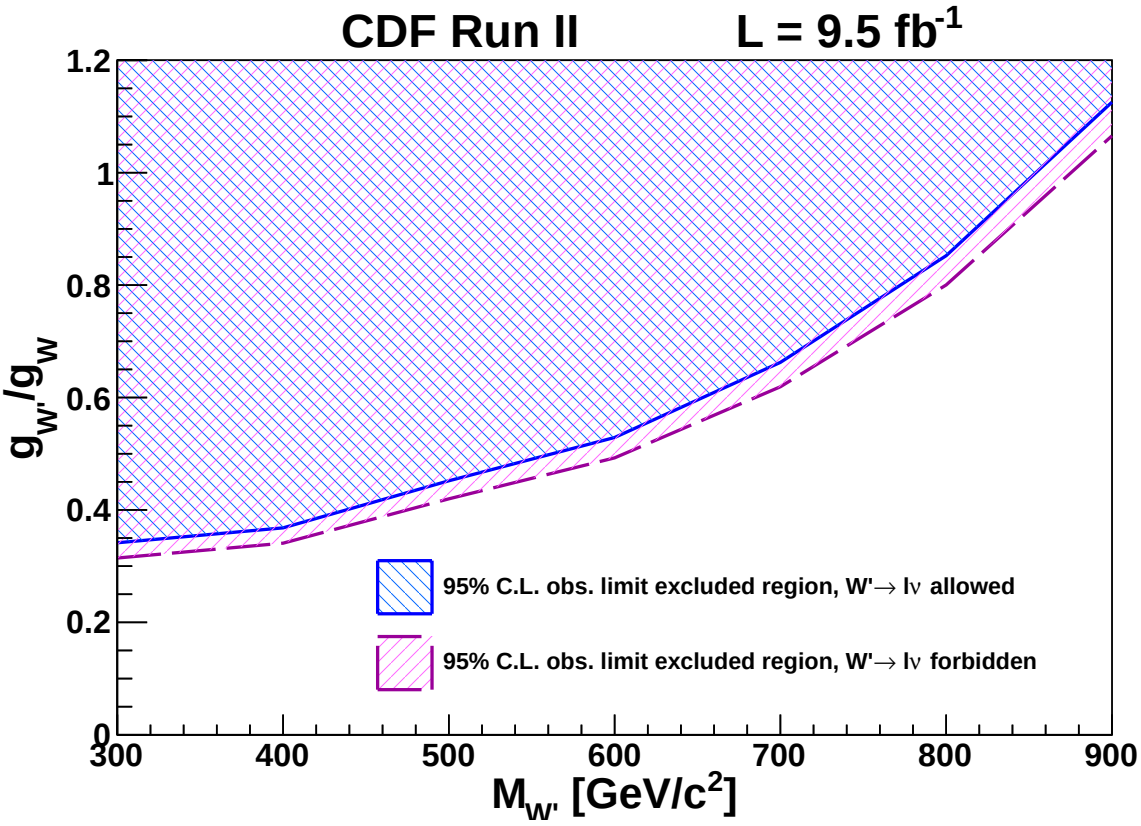

FIG. 4. Observed 95% C.L. limits on the coupling strength of a right-handed W' compared to the SM W boson coupling, $g_{W'}/g_{\rm SM}$, as a function of $M_{W'}$ in cases where the leptonic decay mode $W' \to \ell\nu$ is allowed or forbidden. The patterned region above each line is excluded.

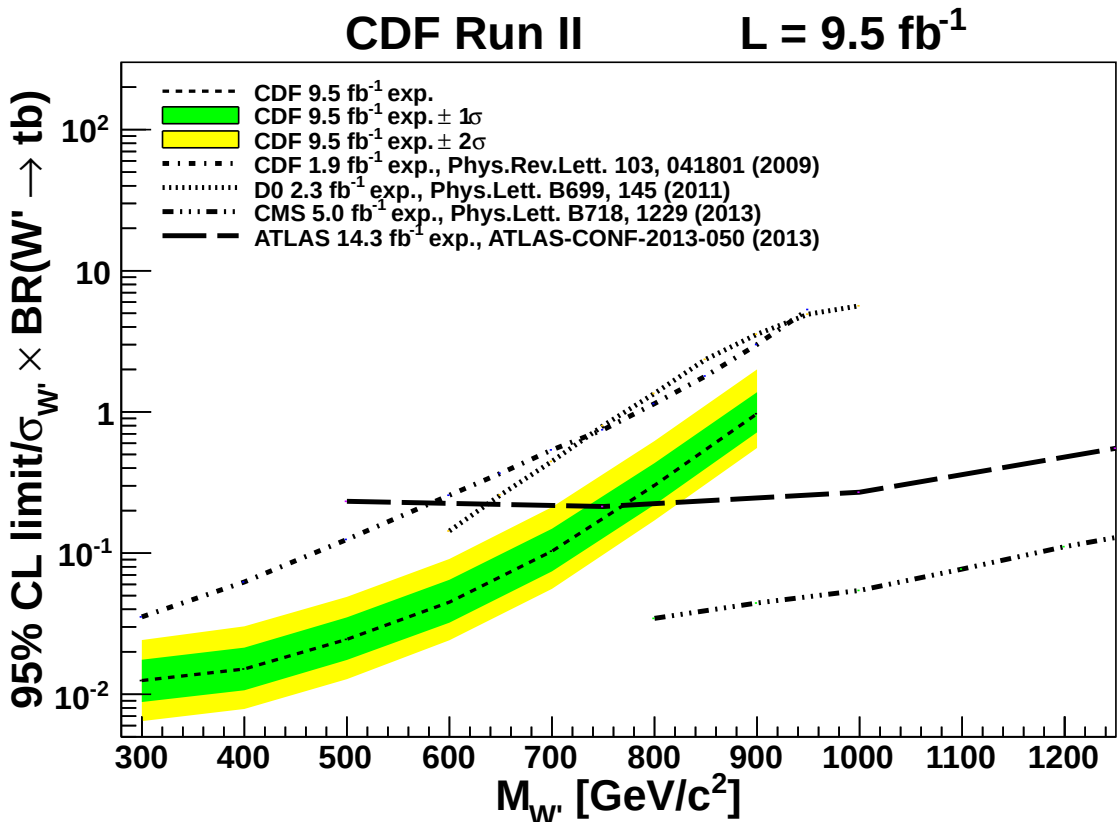

FIG. 5. Expected 95% C.L. limits on the coupling strength of a right-handed W', normalized to the theoretical cross section times branchig ratio as a function of $M_{W'}$ in cases where the leptonic decay mode $W' \to \ell\nu$ is forbidden. The CDF limits are compared with limits from the latest W' searches from ATLAS, CMS and D0 and with precious CDF results.

We thank the Fermilab staff and the technical staffs of the participating institutions for their vital contributions. This work was supported by the U.S. Department of Energy and National Science Foundation; the Italian Istituto Nazionale di Fisica Nucleare; the Ministry of Education, Culture, Sports, Science and Technology of Japan; the Natural Sciences and Engineering Research Council of Canada; the National Science Council of the Republic of China; the Swiss National Science Foundation; the A.P. Sloan Foundation; the Bundesministerium für Bildung und Forschung, Germany; the Korean World Class University Program, the National Research Foundation of Korea; the Science and Technology Facilities Council and the Royal Society, United Kingdom; the Russian Foundation for Basic Research; the Ministerio de Ciencia e Innovación, and Programa Consolider-Ingenio 2010, Spain; the Slovak R&D Agency; the Academy of Finland; the Australian Research Council (ARC); and the EU community Marie Curie Fellowship Contract No. 302103.

[1] J. C. Pati and A. Salam, Phys.Rev. **D10**, 275 (1974)

[2] Y. Mimura and S. Nandi, Phys.Lett. **B538**, 406 (2002)

[3] G. Burdman, B. A. Dobrescu, and E. Ponton, Phys.Rev. **D74**, 075008 (2006)

[4] H. Georgi, E. E. Jenkins, and E. H. Simmons, Nucl.Phys. **B331**, 541 (1990)

[5] E. Malkawi, T. M. Tait, and C. Yuan, Phys.Lett. **B385**, 304 (1996)

[6] M. Perelstein, Prog.Part.Nucl.Phys. **58**, 247 (2007)

[7] T. Aaltonen *et al.* (CDF Collaboration), Phys.Rev.Lett. **103**, 041801 (2009)

[8] V. M. Abazov *et al.* (D0 Collaboration), Phys.Lett. **B699**, 145 (2011)

[9] G. Aad *et al.* (ATLAS Collaboration), Phys.Rev.Lett. **109**, 081801 (2012)

[10] S. Chatrchyan *et al.* (CMS Collaboration), Phys.Lett. **B718**, 1229 (2013)

[11] Z. Sullivan, Phys. Rev. D **66**, 075011 (2002)

[12] D. Acosta *et al.* (CDF Collaboration), Phys.Rev. **D71**, 032001 (2005)Phys.Rev. **D71**, 052002 (2005)

[13] K. J. Potamianos, (2011)

[14] T. Aaltonen *et al.* ((CDF Collaboration)), Phys. Rev. Lett. **112**, 231805 (2014)

[15] A. Bhatti *et al.* (CDF Collaboration), Nucl.Instrum.Meth. **A566**, 375 (2006)

[16] C. Adloff *et al.* (H1 Collaboration), Z.Phys. **C74**, 221 (1997)

[17] We use coordinates where ϕ is the azimuthal angle, θ is the polar angle with respect to the proton beam axis, transverse energy is $E_{\rm T} = E\sin(\theta)$, and the pseudorapidity is $\eta = -\ln[\tan(\theta/2)]$.

[18] A. Abulencia *et al.* (CDF Collaboration), Phys.Rev. **D74**, 072006 (2006)

[19] M. L. Mangano, M. Moretti, F. Piccinini, R. Pittau, and A. D. Polosa, JHEP **0307**, 001 (2003)

[20] M. L. Mangano, M. Moretti, F. Piccinini, and M. Treccani, JHEP **0701**, 013 (2007)

[21] J. Alwall, S. Hoche, F. Krauss, N. Lavesson, L. Lonnblad, *et al.*, Eur.Phys.J. **C53**, 473 (2008)

[22] S. Alioli, P. Nason, C. Oleari, and E. Re, JHEP **1006**, 043 (2010)

[23] T. Sjostrand, S. Mrenna, and P. Z. Skands, JHEP **0605**, 026 (2006)

[24] H. Lai *et al.* (CTEQ Collaboration), Eur.Phys.J. **C12**, 375 (2000)

[25] T. Aaltonen *et al.* (CDF Collaboration), Phys.Rev. **D82**, 034001 (2010)

[26] R. Brun, F. Carminati, and S. Giani, CERN **W5013** (1994)

[27] N. Kidonakis, Phys.Rev. **D81**, 054028 (2010)

[28] J. M. Campbell and R. K. Ellis, Phys.Rev. **D60**, 113006 (1999)

[29] J. Baglio and A. Djouadi, JHEP **1010**, 064 (2010)

[30] P. Baernreuther, M. Czakon, and A. Mitov, , 399 (2012)

[31] T. Aaltonen *et al.* (CDF Collaboration), Phys.Rev.Lett. **110**, 071801 (2013)

[32] T. Aaltonen *et al.* (CDF Collaboration), Phys.Rev. **D82**, 112005 (2010)

[33] D. Acosta *et al.* (CDF Collaboration), Phys.Rev. **D71**, 052003 (2005)

[34] A. Abulencia *et al.* (CDF Collaboration), Phys.Rev. **D74**, 072006 (2006)

[35] T. Aaltonen *et al.* (CDF Collaboration), Phys.Rev.Lett. **109**, 111805 (2012)

[36] M. Bentivegna, Q. Liu, F. Margaroli, and K. Potamianos, (2012), arXiv:1205.4470 [hep-ex]

[37] The event sphericity is defined by $S = \frac{3}{2}(\lambda\_2 + \lambda\_3)$, where the sphericity tensor is $S^{\alpha\beta} = (\sum \_ip\_i^{\alpha} p\_i^{\beta})/(\sum \_ip\_i^2)$ and $\lambda\_1 > \lambda\_2 > \lambda\_3$ are its three eigenvalues and satisfy $\lambda\_1 + \lambda\_2 + \lambda\_3 = 1$. The index i refers to each jet in the event.

[38] K. Nakamura *et al.* (Particle Data Group), J.Phys. **G37**, 075021 (2010)